Available online at www.sciencedirect.com
ScienceDirect
Journal of Catalysis 246 (2007) 35–39
JOURNAL OF CATALYSIS
www.elsevier.com/locate/jcat

The effect of support morphology on the activity of HZSM-5-supported molybdenum catalysts for the aromatization of methane

Alper Sarıoğlan [a,1], Ömer Tunç Savaşçı [b], Ayşe Erdem-Şenatalar [c,*], Alain Tuel [a], Gilbert Sapaly [a], Younès Ben Taârit [a]

[a] *Institut des Recherches sur la Catalyse, C.N.R.S., 69626, Vileurbanne cedex, France*
[b] *Materials and Chemical Technologies Research Institute, TUBITAK Marmara Research Center, P.K. 21, 41470 Gebze/Kocaeli, Turkey*
[c] *Department of Chemical Engineering, İstanbul Technical University, Maslak, 34469 İstanbul, Turkey*

Received 27 June 2006; revised 3 October 2006; accepted 4 October 2006

Available online 19 December 2006

Abstract

The aromatization of methane was investigated over Mo_2C supported on several HZSM-5 zeolites with different morphologies and Si/Al ratios. X-ray diffraction, elemental analyses, X-ray photoelectron spectroscopy, ^{27}Al NMR spectroscopy, nitrogen adsorption, and scanning electron microscopy were used to characterize the supports. Support morphology was observed to play a crucial role in this reaction, which was studied under conditions in which actual rates could be compared. Although rates did not vary linearly either with the total number of the acid sites or with the external surface area, turnover frequencies of the surface acid sites, calculated using the Si/Al ratios determined from XPS measurements, were observed to vary linearly with the external surface area.

Keywords: Aromatization; Methane; Molybdenum; Si/Al ratio; Morphology; External surface

1. Introduction

Conversion of methane into useful chemicals has been and still is a subject of renewed efforts worldwide. Several routes have been explored over the previous two decades. In addition to methane conversion into syngas, which is of real industrial significance, more ambitious routes, such as direct conversion into oxygenates [1–4], methanation of olefins [5], oxidative coupling of methane [6–9], and conversion of methane into benzene and hydrogen, have been explored [10–29].

The latest developments were concerned with the latter reaction carried out in the presence of various transition-metal oxide-loaded inorganic carriers. Mainly molybdenum- and rhenium-based active components deposited over HZSM-5 were thoroughly investigated [22–29].

In the case of molybdenum-based catalysts, the activation procedure was scrutinized, and whatever the nature of the precursor, molybdenum was converted, in the presence of methane, under the reaction conditions, into molybdenum carbide [12,13,24]. Quite recently, Derouane and colleagues showed that it is possible to synthesize bulk or supported metastable fcc molybdenum carbide with a formula MoC_{1-x}. HZSM-5-supported fcc carbide exhibited higher activity and stability and selectivity to benzene in the dehydrocyclization of methane than the hexagonal β-Mo_2C [30–32].

As far as the reaction was concerned, it proceeded via the formation of C_2H_2 (or C_2H_4) over the molybdenum carbide species, acting both as dehydrogenating and coupling functions to create the first C–C bond, and further cyclization and aromatization occurring on the support acid sites. In addition to benzene, a number of aromatics, including xylene, divinylbenzene, and naphthalene, were produced after successive alkylation of benzene by the C_2 intermediate. Higher aromatics and carbon issued from the simple decomposition of methane to its elements escaped direct analysis, although a number of studies

* Corresponding author. Fax: +90 212 285 2925.
E-mail address: aerdem@itu.edu.tr (A. Erdem-Şenatalar).
[1] Present address: Energy Institute, TUBITAK Marmara Research Center, P.K. 21, 41470 Gebze/Kocaeli, Turkey.

0021-9517/$ – see front matter
doi:10.1016/j.jcat.2006.10.005

have been aimed at probing their nature, mode of formation, and identifying their location [33,34].

Although the effect of Mo loading on the activity of HZSM-5-supported catalysts has been studied in detail, comparatively fewer studies have been concerned with the effect of the number of the acid sites [21,28]. Even fewer studies have been devoted to the influence of the support morphology despite its obvious influence on the growth and location of the molybdenum carbide and on the growth and location of the coke precursors in this reaction, in which diffusion of the products likely determines the selectivity among the products and the stability of the catalyst.

The aim of this study is to investigate the effect of support morphology on the activity of HZSM-5-supported molybdenum catalyst. We have used three HZSM-5 zeolite samples that differ in their morphology and aluminum content. The supports were characterized by X-ray diffraction (XRD), inductively coupled plasma (ICP), X-ray photoelectron spectroscopy (XPS), ^{27}Al NMR spectroscopy, nitrogen adsorption, and scanning electron microscopy (SEM) analyses.

2. Experimental

The first sample was synthesized from the following synthesis mixture composition:

100 SiO_2:Al_2O_3:10 TPABr:120 NH_4OH:5000 H_2O,

according to the procedure described by Sand et al. [35] at a pH of 11.8. Crystallization was extended for 6 days (144 h) at 177 °C. The Si/Al ratio of the synthesized sample was 54.

The second support sample was synthesized according to the method of Argauer et al. [36], using the following oxide composition:

40 SiO_2:Al_2O_3:11.7 Na_2O:3.5 $(TPA)_2O$:1480 H_2O.

Aluminum sulfate [$Al_2(SO_4)_3{\cdot}18H_2O$, Aldrich], tetrapropylammonium bromide (TPABr, Aldrich), silica (SiO_2, Grace), and demineralized water were the chemicals used in the synthesis. A 10-g sample of $Al_2(SO_4)_3{\cdot}18H_2O$ was dissolved in 120 ml of water, and 16 g of TPABr was dissolved in 100 ml of water. These two solutions were combined together. Then 36 g of SiO_2 was dissolved at about 60 °C in the caustic solution prepared by adding 14 g of NaOH to 180 ml of water. The mixture of aluminum and template solutions was poured into the silica solution under agitation. The measured pH of the new solution was 11.45. The pH of the solution was adjusted with 50% concentrated H_2SO_4 solution until gel formation occurred. The measured pH of the gel was 10.6. The synthesis mixture was then left to crystallize for 24 h at 170 °C in a Teflon container placed in an autoclave. After synthesis, the ZSM-5 sample was washed until the pH of the washing water was about 7. The washed sample was dried at 100 °C overnight and calcined first under a N_2 flow at 500 °C for 24 h and then under O_2 at 500 °C for 24 h to remove the organic template. The Si/Al ratio of the synthesized sample was 14.

The third sample was supplied by Sud-Chemie AG Mûnchen under reference 1.01 H-MFI granulate SN 130 H/99. This sample had a Si/Al ratio of 28.

The wet-impregnation method was used to load the supports with molybdenum. Ammonium molybdate [$(NH_4)_2MoO_4$ from Touzart & Matignon] was dissolved in a minimum volume of deionized water, and the zeolite was added to the solution so as to achieve a nominal molybdenum content of 4% by weight. The slurry was subsequently dried at 110 °C. Chemical analyses confirmed the actual molybdenum contents to be 3.9% by weight for all three zeolites.

Chemical analyses were performed using inductively coupled plasma spectroscopy (AES-ICP Spectroflame-ICP model D). XRD measurements were carried out using a Bruker D 5005 diffractometer and CuK_α radiation. The 2θ angles were scanned stepwise (0.020°) from 3° to 50°. ^{27}Al NMR spectra of the samples were obtained on a Bruker DSX 400 equipped with a magic-angle spinning probe head operating at room temperature. XPS measurements were performed on a VG Scientific ESCALAB 200 R spectrometer. SEM was done on a Hitachi S 800. Finally, nitrogen adsorption experiments were carried out at −196 °C on a Micrometrics ASAP 2010 system. Samples were evacuated at 300 °C before the adsorption measurements.

A 300-mg sample of the dry catalyst powder was placed in a U-shaped quartz reactor (14 mm i.d.), activated in dry air at 650 °C, and then purged by argon flow (Air Liquide UP) at the same temperature for 30 min.

For precarburization in the presence of CH_4 and H_2, a gas mixture with a CH_4:H_2 ratio of 0.42:10.2 (both in L/h^{-1}) was flown over the catalyst bed for 5 h at 700 °C. After the precarburization step, the catalyst bed was purged with argon at the same temperature for 30 min. In the reactions, 0.42 L/h of methane was diluted with argon to obtain a total flow rate of 13 L/h, resulting in a methane partial pressure of 3.28 kPa in the CH_4/argon mixture.

Products were analyzed in line using three gas chromatographs, two of them equipped with flame ionization detectors and columns packed with unibeads 35 to analyze aliphatics and with bentone to analyze aromatics. The third chromatograph, equipped with a thermal conductivity cell detector and a column packed with carbosieve S, was devoted to the analysis of CO, CO_2, and (mainly) H_2.

The rate of CH_4 conversion to hydrocarbons (benzene, naphthalene, and ethylene) in mol CH_4/(s mol Mo) was calculated from the following equation:

$$r_{\mathrm{HC}} = F_{\mathrm{CH_4,inlet}} X_{\mathrm{CH_4\ to\ HC}} (1/n_{\mathrm{Mo}}), \tag{1}$$

where $F_{\mathrm{CH_4,inlet}}$ is the total inlet molar flow rate of CH_4 in mol/s, $X_{\mathrm{CH_4\ to\ HC}}$ is the CH_4 conversion to hydrocarbon products (namely benzene, naphthalene, and ethylene), and n_{Mo} is the number of moles of molybdenum atoms present on the catalyst sample. CH_4 conversion to hydrocarbon products ($X_{\mathrm{CH_4\ to\ HC}}$) was calculated from the partial pressures of the hydrocarbons formed based on the measured GC responses, reaction stoichiometries, and the differential reactor assumption, as $P_{\mathrm{CH_4\ to\ HC}}/P_{\mathrm{CH_4,inlet}}$.

Table 1
Characterization results of the catalyst supports

Si/Al	Si/Al_{ext}[a]	n_{ext}[b]	S_{micro}[c] (m^2/g)	r_{max}[d]	r_{max}/n_{ext}	S_{ext}[e] (m^2/g)
14	16.7	5.42	400	0.553	0.100	32
28	34.4	2.71	430	0.652	0.240	83
54	54	1.74	350	0.052	0.030	10

[a] Si/Al ratio in the external layers.
[b] Number of acid sites per unit cell in the external layers.
[c] Micropore surface area by N_2 adsorption.
[d] Maximum rate of hydrocarbon formation ($\times 10^{-3}$ mol CH_4/(s mol Mo)).
[e] External surface area calculated using t-plot method.

3. Results and discussion

XRD measurements confirmed the ZSM-5 structure for the support samples and showed that all were highly crystalline. The framework Si/Al ratios of the support samples calculated from the chemical analyses and XPS results are given in Table 1. Absence of extra-framework aluminum species in the samples was confirmed by ^{27}Al NMR analyses.

XPS results indicated that the external layers of two of the support samples were depleted in aluminium compared with the bulk. Except for the sample with the lowest aluminum content, the Si/Al ratios of the other two samples were significantly higher than the overall Si/Al ratio, in line with the general observation that nucleation involves aluminum-rich moieties with respect to the nutrient solution. The number of acid sites per unit cell in the external layers for each of these samples was calculated based on the XPS results; the values are listed in Table 1.

Surface areas of the samples determined from the N_2 adsorption results are also given in Table 1. In agreement with literature reports, micropore area values were within the range of 350–450 m^2/g. The external surface area values determined by the t-plot method, on the other hand, covered a wide range, 10–83 m^2/g.

Typical scanning electron micrographs for the samples are shown in Figs. 1–3. Sample 1, with the lowest aluminum content (Si/Al = 54) exhibited well-defined crystals of the coffin shape with an average length of 35–45 μm, a width of 12–15 μm, and a thickness of 8 μm, as shown in Fig. 1. Quite often these crystal were twinned. Sample 2, from Sud-Chemie (Si/Al = 28), exhibited a very uniform morphology composed mainly of very small individual crystals that agglomerate into small ensembles, leaving small open spaces and larger voids, with a 2–3 micron diameter, giving the picture of an eroded sponge, as shown in Fig. 2. These arrangements of the submicron agglomerates well account for the observed high external surface area and high mesopore volume.

The micrograph of sample 3, the richest in aluminum (Si/Al = 14), is quite different. The large agglomerates vary in diameter from 0.5 micron to about 7 microns (Fig. 3). These cauliflower-like larger particles are made up of much smaller lamellar-type crystals in the 0.1–0.3 μm size range. There is nothing like the large voids in the 2–3 μm range encountered in the case of the previous sample. Such morphology is in agreement with the measured external (or mesoporous) volume or

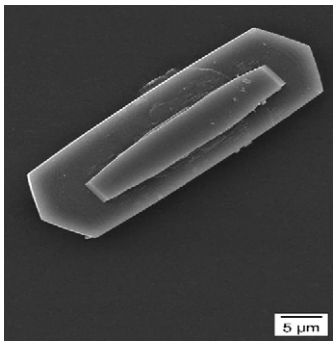

Fig. 1. SEM picture of the ZSM-5 sample with a Si/Al ratio of 54 or sample 1.

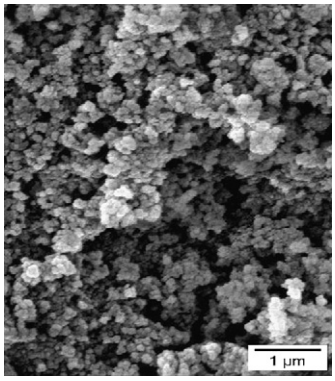

Fig. 2. SEM picture of the ZSM-5 sample with a Si/Al ratio of 28 or sample 2.

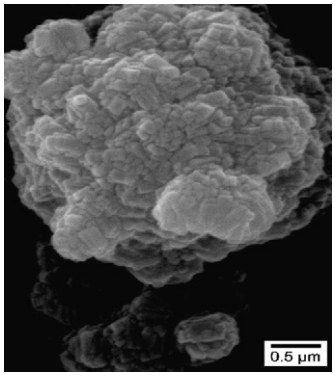

Fig. 3. SEM picture of the ZSM-5 sample with a Si/Al ratio of 14 or sample 3.

surface area of this sample, which was observed to be lower with respect to the sample from Sud Chemie (sample 2), but higher than that of the highest silica sample (sample 1).

These three solids were loaded with molybdenum and tested as catalyst supports in the aromatization of methane under the conditions specified in the previous section. The rates of methane conversion into hydrocarbons varied with time on stream in a generally similar manner, as shown in Fig. 4. An initial increase in activity was observed in all cases followed by a maximum, which was rather sharp for two of the samples. An almost symmetric decline of the rate was then followed by a slower but continuous deactivation. The maximum rates are also reported in Table 1.

We compared the maximum rates in an effort to relate them to the number of aluminum atoms per unit cell in the external

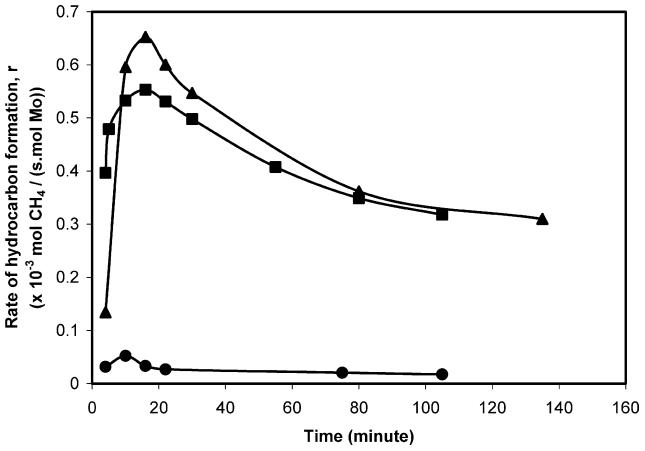

Fig. 4. Variation of the rate of hydrocarbon formation with time on stream for the catalysts supported on ZSM-5 of (■) Si/Al = 14; (▲) Si/Al = 28; (●) Si/Al = 54.

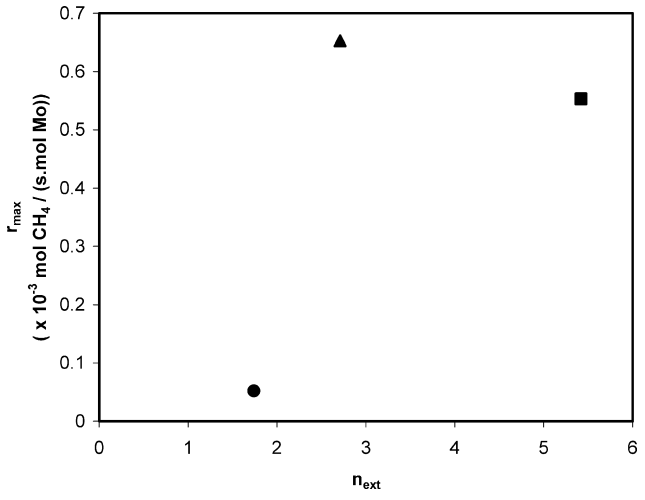

Fig. 5. Variation of the maximum rate of hydrocarbon formation, r_{max}, with the number of acid sites per unit cell in the external layers, n_{ext}, for the catalysts supported on ZSM-5 of (■) Si/Al = 14; (▲) Si/Al = 28; (●) Si/Al = 54.

layers. The plot shown in Fig. 5 is far from the linear variation expected for a reaction having acidity as the rate-determining function. The activity was shown not to vary with the molybdenum content beyond a value of 3.5–4%.

In a further attempt to relate the activity to the morphological data of these catalysts, the maximum rates were plotted against the external surface areas. The results are shown in Fig. 6. Here an increase of the rate was observed with increasing external surface, although there was no linear relationship between the two.

Finally, the rate could well be a function of both the external acid site density and the available external surface, obeying a relation of the form

$$R = knS_{ext},$$

where n is the number of acid sites per unit cell in the external layers and S_{ext} is the external surface area.

The result of this attempt to relate the rate to both the external surface area and the acid site density is shown in Fig. 7,

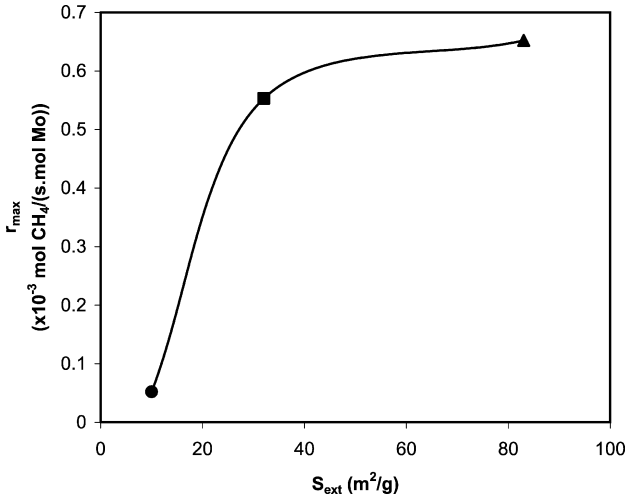

Fig. 6. Variation of the maximum rate of hydrocarbon formation, r_{max}, with the external surface area, S_{ext}, for the catalysts supported on ZSM-5 of (■) Si/Al = 14; (▲) Si/Al = 28; (●) Si/Al = 54.

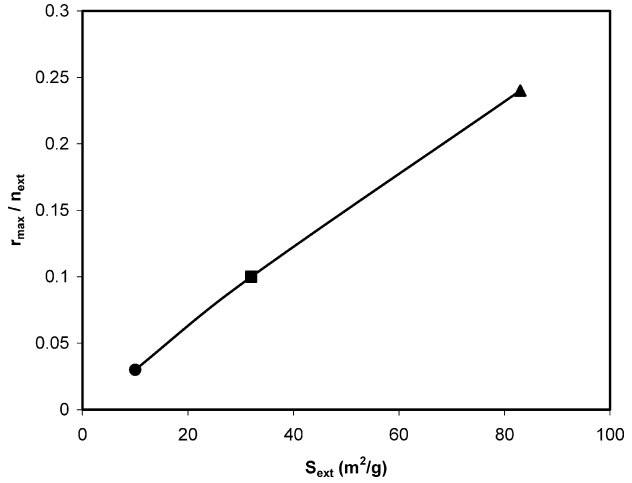

Fig. 7. Variation of the ratio of maximum rate of hydrocarbon formation to the number of acid sites per unit cell in the external layers (r_{max}/n_{ext}) with the external surface area, S_{ext}, for the catalysts supported on ZSM-5 of (■) Si/Al = 14; (▲) Si/Al = 28; (●) Si/Al = 54.

where r/n is plotted against S_{ext}. A very decent linear relationship was obtained, confirming the major effect of the external surface area for this reaction. Clearly, most of the reaction proceeds within the external layers, if not exclusively at the external surfaces. This is not unexpected at these high space velocities and high temperatures. Transport phenomena very often determine the efficiency of the catalyst even in the case of molecules as small as methane and water, as in methane steam reforming [37,38].

4. Conclusion

The aromatization of methane was carried out over molybdenum carbide supported on three HZSM-5 samples with differing aluminum contents and morphologies. These samples, two of which were synthesized in the course of this work, were characterized based on their morphologies, structures, and sur-

face compositions. The rates of conversion of methane into hydrocarbons appeared to not vary simply with the number of acid sites, as is usually expected. Rather, they depended on this variable together with the accessible external surface area, clearly indicating that transport phenomena were determining the overall rate. A high external surface area appeared to be a prerequisite for efficient catalysts, as implied from the linear relationship observed between the turnover frequency and the external surface area.

Acknowledgments

A.S. acknowledges the funding provided by TUBITAK MRC via the World Bank Program, which covered all his expenses during his stay at Institut de Recherches sur la Catalyse, France.

References

[1] G. Koenig, D.O.S. 3 101 024, 1982.
[2] O.T. Onsager, R. Lodeng, P. Soraker, A. Anundskaas, B. Helleborg, Catal. Today 4 (1989) 355.
[3] K. Otsuka, M.J. Hatano, J. Catal. 108 (1987) 252.
[4] M.A. Banares, B. Pawelee, J.L.G. Fierro, Zeolites 12 (1992) 882.
[5] M.S. Scurrell, Appl. Catal. 34 (1987) 109.
[6] G.E. Keller, M.M. Bhasin, J. Catal. 73 (1982) 9.
[7] T. Ito, J.H. Lunsford, Nature 314 (1982) 9.
[8] T. Ito, J.X. Wang, C.H. Lin, J.H. Lunsford, J. Am. Chem. Soc. 107 (1985) 5062.
[9] L. Wang, L. Tao, M. Xie, G. Xu, J. Huang, Y. Xu, Catal. Lett. 21 (1993) 35.
[10] Y. Xu, S. Liu, L. Wang, M. Xie, X. Guo, Catal. Lett. 30 (1995) 135.
[11] F. Solymosi, A. Erdohelyi, A. Szoke, Catal. Lett. 32 (1995) 43.
[12] D. Wang, J.H. Lunsford, M.P. Rosynek, Top. Catal. 3 (1996) 289.
[13] D. Wang, J.H. Lunsford, M.P. Rosynek, J. Catal. 169 (1997) 347.
[14] F. Solymosi, J. Cserenyi, A. Szoke, T. Bansagi, A. Oszko, J. Catal. 165 (1997) 150.
[15] B.M. Weckhuysen, D. Wang, M.P. Rosynek, J.H. Lunsford, J. Catal. 175 (1998) 338.
[16] S. Liu, Q. Dong, R. Ohnishi, M. Ichikawa, Chem. Commun. (1998) 1217.
[17] P. Mériaudeau, L.V. Tiep, V.T.T. Ha, C. Naccache, G. Szabo, J. Mol. Catal. 144 (1999) 469.
[18] P. Mériaudeau, V.T.T. Ha, L.V. Tiep, Catal. Lett. 64 (2000) 49.
[19] S. Liu, L. Wang, R. Ohnishi, M. Ichikawa, J. Catal. 181 (1999) 175.
[20] R.M. Borry, H.Y. Kim, A. Huffsmith, J.A. Reimer, E. Iglesia, J. Phys. Chem. B 103 (1999) 5787.
[21] W. Ding, G.D. Meitzner, E. Iglesia, J. Catal. 206 (2002) 14.
[22] W. Zhang, D. Ma, X. Han, X. Liu, X. Bao, X. Guo, X. Wang, J. Catal. 188 (1999) 393.
[23] D. Ma, Y. Shu, M. Cheng, Y. Xu, W. Bao, J. Catal. 194 (2000) 105.
[24] W. Ding, S. Li, G.D. Meitzner, E. Iglesia, J. Phys. Chem. B 105 (2001) 506.
[25] L. Wang, R. Ohnishi, M. Ichikawa, Catal. Lett. 62 (1999) 29.
[26] L. Wang, R. Ohnishi, M. Ichikawa, J. Catal. 190 (2000) 276.
[27] J.S. Lee, S.T. Oyama, M. Boudart, J. Catal. 106 (1987) 125.
[28] A. Sarıoğlan, A. Erdem-Şenatalar, O.T. Savaşçı, Y. Ben Taârit, J. Catal. 226 (2004) 210.
[29] A. Sarıoğlan, A. Erdem-Şenatalar, O.T. Savaşçı, Y. Ben Taârit, J. Catal. 228 (2004) 114.
[30] C. Bouchy, S.B. Derouane-Abd Hamid, E.G. Derouane, Chem. Commun. 2 (2000) 125.
[31] C. Bouchy, I. Schmidt, J.R. Anderson, C.J.H. Jacobsen, E.G. Derouane, S.B. Derouane-Abd Hamid, J. Mol. Catal. 163 (2000) 283.
[32] S.B. Derouane-Abd Hamid, J.R. Anderson, I. Schmidt, C. Bouchy, C.J.H. Jacobsen, E.G. Derouane, Catal. Today 63 (2000) 461.
[33] B.M. Weckhuysen, M.P. Rosynek, J.H. Lunsford, Catal. Lett. 52 (1998) 31.
[34] H. Jiang, L. Wang, W. Cui, Y. Xu, Catal. Lett. 57 (1999) 95.
[35] A. Nastro, L.B. Sand, Zeolite 3 (1983) 57.
[36] R.G. Argauer, G.R. Landolt, US Patent 3 702 886, 1972.
[37] J.R. Rostrup-Nielsen, in: J.R. Anderson, M. Boudart (Eds.), Catalysis Science and Technology, vol. 5, Springer, Berlin, 1984, chap. 1.
[38] J.R. Rostrup-Nielsen, L.J. Christiansen, J.H. Back Hansen, Appl. Catal. 43 (1988) 287.